



## Cyclopropyl- and methyl-containing inhibitors of neuronal nitric oxide synthase



Huiying Li<sup>a,b,c</sup>, Fengtian Xue<sup>d,e,†</sup>, James M. Kraus II<sup>d,e</sup>, Haitao Ji<sup>d,e,‡</sup>, Kristin Jansen Labby<sup>d,e</sup>, Jan Mataka<sup>d,e,§</sup>, Silvia L. Delker<sup>a,b,c,¶</sup>, Pavel Martásek<sup>f,g</sup>, Linda J. Roman<sup>f</sup>, Thomas L. Poulos<sup>a,b,c,\*</sup>, Richard B. Silverman<sup>d,e,\*</sup>

<sup>a</sup> Department of Molecular Biology and Biochemistry, University of California, Irvine, CA 92697-3900, United States

<sup>b</sup> Department of Pharmaceutical Chemistry, University of California, Irvine, CA 92697-3900, United States

<sup>c</sup> Department of Chemistry, University of California, Irvine, CA 92697-3900, United States

<sup>d</sup> Department of Chemistry, Chemistry of Life Processes Institute, Center for Molecular Innovation and Drug Discovery, Northwestern University, 2145 Sheridan Road, Evanston, IL 60208-3113, United States

<sup>e</sup> Department of Molecular Biosciences, Chemistry of Life Processes Institute, Center for Molecular Innovation and Drug Discovery, Northwestern University, 2145 Sheridan Road, Evanston, IL 60208-3113, United States

<sup>f</sup> Department of Biochemistry, University of Texas Health Science Center, San Antonio, TX, United States

<sup>g</sup> Department of Pediatrics, 1st School of Medicine, Charles University, Prague, Czech Republic

### ARTICLE INFO

#### Article history:

Received 31 October 2012

Revised 4 December 2012

Accepted 12 December 2012

Available online 22 December 2012

#### Keywords:

Neuronal nitric oxide synthase

Inhibition

Isozyme selectivity

Cyclopropyl analogues

X-ray crystallography

### ABSTRACT

Inhibitors of neuronal nitric oxide synthase have been proposed as therapeutics for the treatment of different types of neurological disorders. On the basis of a *cis*-3,4-pyrrolidine scaffold, a series of *trans*-cyclopropyl- and methyl-containing nNOS inhibitors have been synthesized. The insertion of a rigid electron-withdrawing cyclopropyl ring decreases the basicity of the adjacent amino group, which resulted in decreased inhibitory activity of these inhibitors compared to the parent compound. Nonetheless, three of them exhibited double-digit nanomolar inhibition with high nNOS selectivity on the basis of *in vitro* enzyme assays. Crystal structures of nNOS and eNOS with these inhibitors bound provide a basis for detailed structure–activity relationship (SAR) studies. The conclusions from these studies will be used as a guide in the future development of selective NOS inhibitors.

© 2012 Elsevier Ltd. All rights reserved.

### 1. Introduction

Nitric oxide (NO) has a wide variety of functions in the body, the most well-studied of which are its regulatory action on smooth muscle relaxation, cytotoxic activity in the immune system, neurotransmission, brain development and protection, and maintenance of synaptic plasticity.<sup>1</sup> The production of NO is mediated via the activity of nitric oxide synthase (NOS),<sup>2,3</sup> a family of homodimeric heme-containing monooxygenases, which metabolizes L-arginine

and O<sub>2</sub> to L-citrulline and NO.<sup>4</sup> A considerable body of research has shown that overproduction of cerebral NO by the neuronal isoform of NOS (nNOS) is a general pathological phenomenon for various neurological disorders such as Parkinson's,<sup>5</sup> Alzheimer's,<sup>6</sup> Huntington's,<sup>7</sup> headaches,<sup>8</sup> and cerebral palsy.<sup>5–10</sup> This has led to the search for and development of selective inhibitors of nNOS over endothelial NOS (eNOS), the isozyme that is responsible for the regulation of blood pressure, and inducible NOS (iNOS), the isozyme that is critical for immune responses, as therapeutic agents for the treatment of neurological disorders.<sup>11</sup>

In our on-going effort to develop novel nNOS inhibitors, we recently reported a series of *cis*-3,4-pyrrolidine-based inhibitors.<sup>12–14</sup> In this family, several inhibitors have shown remarkable neuroprotective properties in a preclinical rabbit model for cerebral palsy.<sup>13</sup> Compound **1**, as an example, not only is neuroprotective but is the most selective nNOS inhibitor over eNOS and iNOS yet reported.<sup>14</sup> Despite its promising inhibitory activity, further application of **1** has been impeded by several of its structural characteristics. First, the flexible *m*-fluorophenyl ethanamino tail produces multiple rotatable bonds in the inhibitor. In addition, the benzylic position

\* Corresponding authors. Tel.: +1 949 824 7020 (T.L.P.); tel.: +1 847 491 5653 (R.B.S.).

E-mail addresses: [poulos@uci.edu](mailto:poulos@uci.edu) (T.L. Poulos), [Agman@chem.northwestern.edu](mailto:Agman@chem.northwestern.edu) (R.B. Silverman).

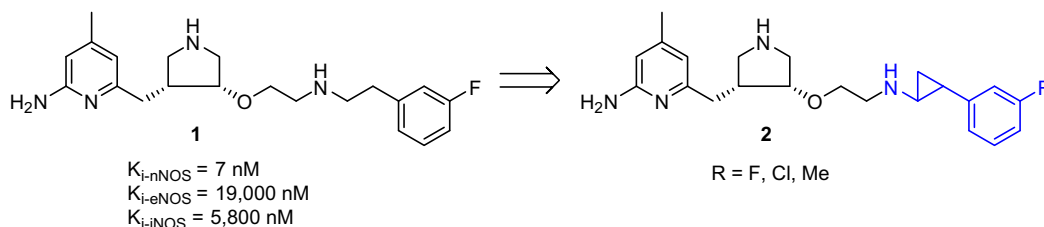
<sup>†</sup> Current address: Department of Pharmaceutical Sciences, University of Maryland School of Pharmacy, 20 North Pine Street, Baltimore, MD 21201, United States.

<sup>‡</sup> Current address: Department of Chemistry, University of Utah, Salt Lake City, UT 84112-0850, United States.

<sup>§</sup> Current address: Department of Chemistry, Northeastern Illinois University, Chicago, IL 60625-4699, United States.

<sup>¶</sup> Current address: Celgene, 4550 Towne Centre Court, San Diego, CA 92121, United States.

of the *m*-fluorophenyl ring is highly susceptible to metabolic oxidation.<sup>15</sup> Also, the two positive charges of **1** at physiological pH, derived from the two secondary amino groups, decreases the chance of **1** to penetrate the blood-brain barrier (BBB).<sup>13</sup> These considerations prompted the development of new pyrrolidine nNOS inhibitors with a potentially more desirable pharmacokinetic and pharmacodynamic profile.



Different strategies have been applied to modify the chemical structure of **1**.<sup>16–20</sup> Herein we describe the design and synthesis of a new series of inhibitors (**2**), with a structurally constrained cyclopropyl ring inserted in the position adjacent to the amino group of the ethanamine tail. Conformational restriction using cyclopropyl fragments is a strategy that has been widely used in modern drug design to create novel inhibitors for a variety of enzymes.<sup>21–23</sup> Introduction of the cyclopropyl group (**2**) can potentially enhance inhibitory activity by stabilizing and thereby reducing the energetic penalty in binding to the enzyme active site and thus improve selectivity.<sup>24,25</sup> In addition, the insertion of a cyclopropyl fragment can block the potential metabolic oxidation at the benzylic position of the *m*-fluorophenyl ring.<sup>15</sup> Furthermore, the electron-withdrawing character of the cyclopropyl ring decreases the basicity of the adjacent amino group. The calculated  $pK_a$  value of the amino group in the lipophilic tail of **2** is  $\sim 7.4$ , which is significantly lower than 8.9 in **1**.<sup>26</sup> As a result, pseudo-monocationic molecule **2** may have improved BBB permeability.<sup>15</sup> Here we report structure–activity relationship studies on these cyclopropyl containing inhibitors to determine if enhanced potency and selectivity can be attained prior to consideration of pharmacokinetic property assessment.

## 2. Chemistry

The key amine building blocks (**3a–e**) were synthesized as shown in Schemes 1 and 2. Starting from 1-substituted-3-vinyl-

benzenes **4a–c**, Rh(II)-catalyzed cyclopropanation produced **5a–c** as *cis/trans* mixtures in good yields.<sup>27</sup> Ethyl esters **5a–c** were treated with NaOCH<sub>3</sub> in refluxing EtOH to induce epimerization, generating the thermodynamically more stable *trans* isomers, which were hydrolyzed in aqueous LiOH to yield **6a–c** in good yields.<sup>27</sup> Carboxylic acids **6a–c** were converted to Boc-protected amines (**7a–c**) through Curtius rearrangement reactions in reasonable

yields.<sup>28</sup> Finally, the Boc-protecting groups of **7a–c** were removed in trifluoroacetic acid (TFA) to provide ( $\pm$ )-*trans*-**3a–c** as TFA salts in high yields (see Scheme 3)

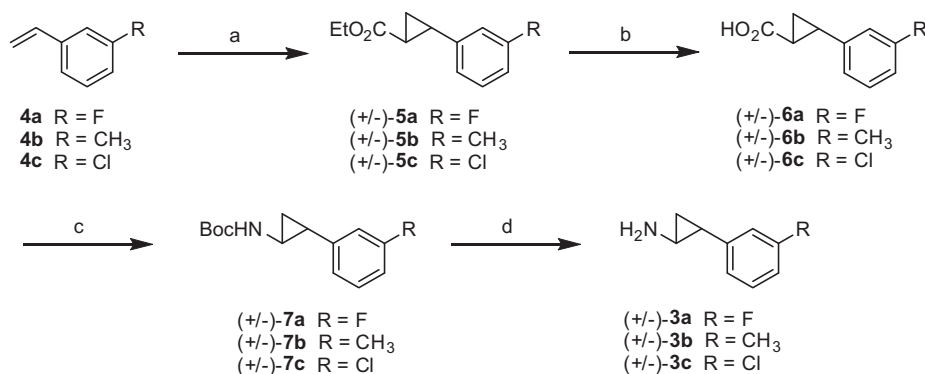
The two enantiomers of **3a** were resolved in two steps. First, **3a** was treated with (*S*)-(-) camphoric chloride in the presence of triethylamine (TEA) to produce two separable diastereomers **8a** and **8b**. Then the amide bonds of **8a** and **8b** were hydrolyzed in concentrated HCl to generate single enantiomers **3d** and **3e** in good yields.

The syntheses of inhibitors **2a–d** began with (*R,R*)-**9a**.<sup>29</sup> Compound **9a** underwent reductive amination with amines **3a–c** and **3e** using NaBH(OAc)<sub>3</sub> as a reducing reagent to generate **10a–d** in good yields. Next, the three Boc-protecting groups of **10a–d** were removed in HCl to yield inhibitors **2a–d** in high yields.

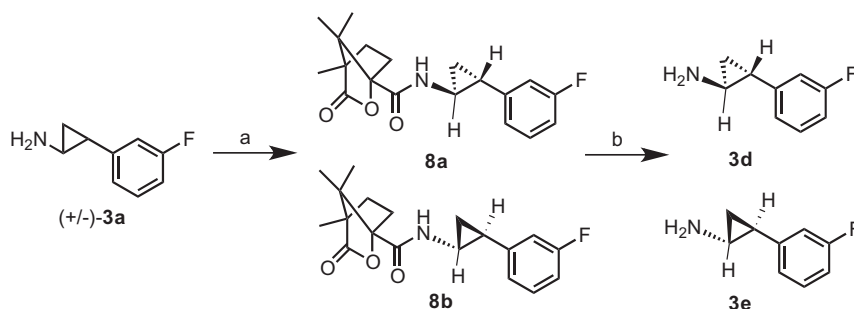
The synthesis of inhibitors **2e,f** began with aldehyde **9b** (Scheme 4).<sup>13</sup> Reductive amination of **9b** with amine **3a** or **3e** provided the corresponding secondary amine, which was further protected with a Boc-protecting group to give **10e,f** in reasonable yields. Next, the cyclopropyl group was reduced, along with deprotection of the Bn-protecting group, by catalytic hydrogenation using Pd(OH)<sub>2</sub> as a catalyst at 60 °C to generate **11e,f**. Finally, the three Boc-protecting groups were removed in HCl to provide inhibitors **2e,f** as tris-HCl salts in good yields.

## 3. Structure–activity studies

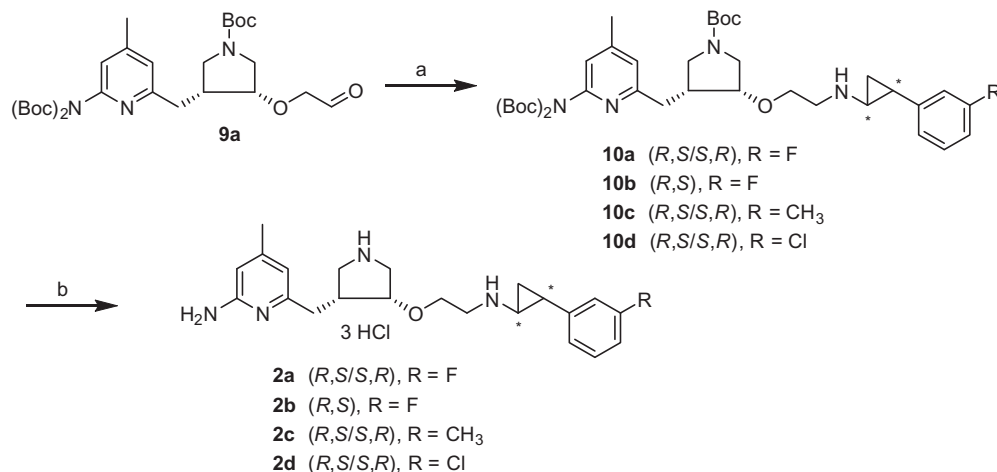
Nitric oxide hemoglobin capture assays were performed with **2a** through **2f** against three NOS isoforms to obtain the in vitro



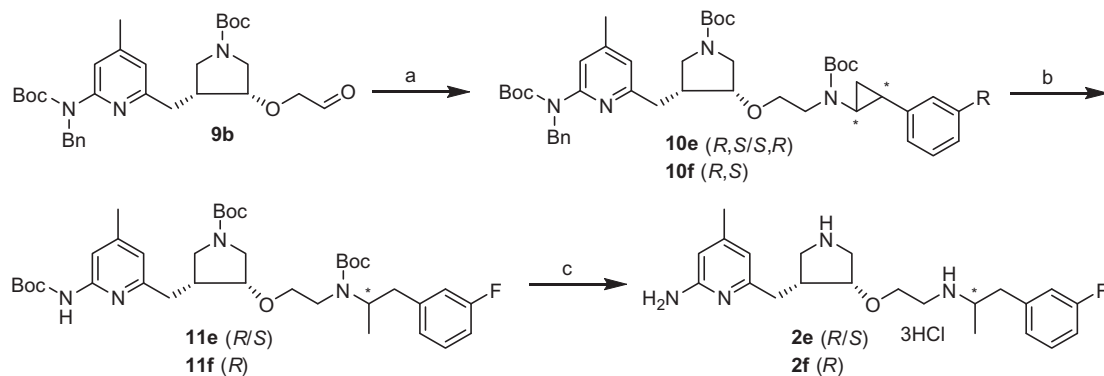
**Scheme 1.** Synthesis of **3a–c**. Reagents and conditions: (a) EtO<sub>2</sub>CCHN<sub>2</sub>, Rh<sub>2</sub>(OAc)<sub>4</sub>, toluene, 80–85 °C, 2 h; (b) (i) NaOCH<sub>3</sub> in EtOH (1 M), reflux, 40 h, (ii) LiOH, MeOH/H<sub>2</sub>O, 70 °C, 16 h, 75–80% for two steps; (c) diphenyl phosphorazidate, triethylamine, *t*-BuOH, 85 °C, 48 h, 75–82%; (d) TFA/CH<sub>2</sub>Cl<sub>2</sub> (1:2), room temp, 45 min.



**Scheme 2.** Resolution of enantiomers **3d** and **3e**. Reagents and conditions: (a) (*S*)-(-)-camphanic chloride,  $\text{CH}_2\text{Cl}_2$ , TEA, room temp, 30 min, 91% for two diastereomers; (b) 12 N HCl, EtOH (2:1), reflux, 72 h, 67–70%.



**Scheme 3.** Synthesis of **2a–d**. Reagents and conditions: (a) amine hydrochloride, TEA,  $\text{NaBH}(\text{OAc})_3$ , room temp, 3 h, 81–87%; (d) 6 N HCl in MeOH (2:1), room temp, 16 h, 90–99%. The *R/S* notations shown indicate the chirality of the two chiral centers of the cyclopropyl ring; the pyrrolidine ring has (*R,R*) stereochemistry in all of the compounds.

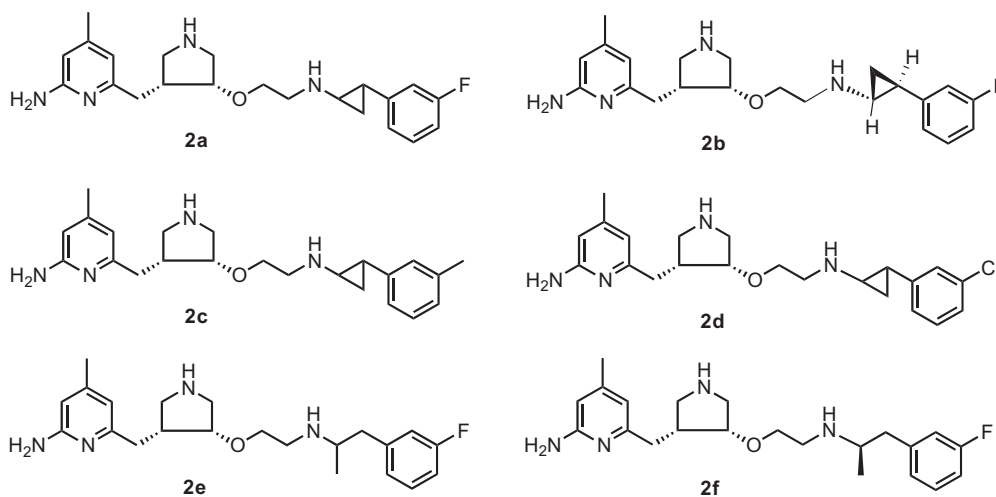


**Scheme 4.** Synthesis of inhibitors **2e–f**. Reagents and conditions: (a) (i) **3a** or **3e**, TEA,  $\text{NaBH}(\text{OAc})_3$ , room temp, 3 h, (ii)  $(\text{Boc})_2\text{O}$ , TEA, MeOH, room temp, 6 h, 60% for two steps; (b)  $\text{H}_2$ ,  $\text{Pd}(\text{OH})_2/\text{C}$ , 60 °C, 30 h; (c) 6 N HCl/MeOH (2:1), room temp, 16 h, 25% for two steps. The *R/S* notations shown indicate the chirality of the two chiral centers of the cyclopropyl ring; the pyrrolidine ring has (*R,R*) stereochemistry in all of the compounds.

inhibitory potency and isoform selectivity for this series of compounds (Table 1). Crystal structures of nNOS and eNOS with these inhibitors bound were also determined, which provides the basis for structure–activity relationship (SAR) studies.

Consistent with the binding mode of (3*R*,4*R*)-**1**,<sup>14</sup> all six inhibitors in this study bind to both nNOS and eNOS in a flipped orientation. As shown in Figure 1, the two nitrogen atoms of aminopyridine donate two hydrogen bonds to heme propionate D. The pyrrolidine ring nitrogen is positioned between heme propionate A and the C=O group of the pterin, thereby forming hydrogen bonds to both. This binding mode leaves the cyclopropyl and phenyl rings of the inhibitor tail right above the heme and provides the primary differences between the **1** and **2** interactions with the local surroundings.

The introduction of a cyclopropyl ring adjacent to the amine in the tail end of the inhibitor was designed to lower the  $\text{pK}_a$  ( $\text{pK}_a = 7.4$ , calculated by ACD/Labs 7.0) of this otherwise basic group (**1**,  $\text{pK}_a = 8.9$ , calculated by ACD/Labs 7.0) to improve membrane permeability of the inhibitor. The rigidity along the inhibitor tail results in the cyclopropyl ring forcing the amino group to face more exclusively toward the active site Glu residue (Glu592 in nNOS or Glu363 in eNOS). This amino group of the inhibitor recruits the Glu residue as its hydrogen-bonding partner, forcing the Glu side chain into an alternate rotamer position (Fig. 1). The alternate Glu side chain rotamer also was observed in the eNOS–**1** complex structure but not in the nNOS–**1** structure.<sup>14</sup> The more flexible tail in **1** allows the amino nitrogen to point in various

**Table 1** $K_i^a$  Values of inhibitors for rat nNOS, bovine eNOS, and murine iNOS

Compound	nNOS ( $\mu\text{M}$ )	eNOS ( $\mu\text{M}$ )	iNOS ( $\mu\text{M}$ )	Selectivity <sup>b</sup>	
				n/e	n/i
( $\pm$ ) <b>2a</b>	0.170	51	16	300	94
<b>2b</b>	0.175	31	12	177	69
( $\pm$ ) <b>2c</b>	0.140	45	10	320	72
( $\pm$ ) <b>2d</b>	0.071	26	0.86	370	12
( $\pm$ ) <b>2e</b>	0.046	68	10.2	1500	220
<b>2f</b>	0.070	40	7.6	570	110

<sup>a</sup> The  $K_i$  values were calculated based on the directly measured  $\text{IC}_{50}$  values, which represent at least duplicate measurements with standard deviations of  $\pm 10\%$ .

<sup>b</sup> The ratio of  $K_i$  (eNOS or iNOS) to  $K_i$  (nNOS).

directions. And, therefore, there is not enough driving force to bring the Glu side chain into an alternate rotamer in nNOS.

We also have tested the impact of chirality at the cyclopropyl ring on inhibitor binding potency. The nNOS complex structures show that when a racemic compound mixture is used in crystal soaking, the 'ring up' (*R,S*) enantiomer binds exclusively (Fig. 1B and C), although the 'ring down' (*S,R*) enantiomer (**2b**) can still bind if it is the only isomer used for crystal soaking (Fig. 1A). The different stereochemistry around the cyclopropyl ring results in slightly different orientations (more than  $12^\circ$ ) for the tail phenyl ring, which is more parallel to the heme plane in the 'ring down' (*S,R*) enantiomer than in the 'ring up' (*R,S*) isomer (Fig. 2A). Moreover, in the 'ring down' (*S,R*) enantiomer both the cyclopropyl (3.1 Å) and phenyl (2.7 Å) rings are farther away from the native Glu592 side chain position and, thus, can tolerate both the native and alternate Glu592 rotamer positions. In contrast, the cyclopropyl or phenyl ring in the 'ring up' (*R,S*) enantiomer, as in **2c** or **2d**, is so close to the native Glu592 side chain, being 2.5 Å to cyclopropyl and 2.3 Å to phenyl ring in **2c** assuming the Glu592 is in its native position, that the alternate Glu592 rotamer is favored (Fig. 1B and C). Therefore, two factors can potentially influence the Glu592 side chain conformation: (1) a H-bond (or salt bridge) with the inhibitor amino group and (2) a steric repulsion between the phenyl ring and Glu592. The cyclopropyl-containing inhibitors reported here either force the amino group to face Glu592 or bring the tail phenyl ring closer to Glu592, resulting in alternate Glu592 side chain conformations.

Overall the 'ring up' (*R,S*) enantiomer fits better into the nNOS active site. The alternate rotamer of Glu592 plays an important role here since in the better binding 'ring up' (*R,S*) mode Glu592 is in a better position to H-bond with the tail amine group of inhibitors **2c** and **2d** (Fig. 1). Another factor to consider is how the halogen/methyl group of the phenyl ring fits into the hydrophobic pocket defined by Val567 and Phe584 (Fig. 1). The larger methyl group and chloro atom relative to the smaller fluoro atom pushes the

phenyl ring about 0.5 Å closer to Glu592, which forces Glu592 to adopt primarily the alternate rotamer conformation. As noted earlier, this alternate rotamer makes a better hydrogen bond with the inhibitor. Therefore, it is both the size of the substituent attached to the phenyl ring and the chirality of the inhibitor that contribute to differences in binding affinity. It is probably the resulting difference in hydrogen bond strength from the tail amino group to the alternate Glu592 side chain position that is the main reason why **2d** shows a two-fold better binding affinity to nNOS than that of either **2a** or **2c** (Table 1).

Introduction of a cyclopropyl ring next to the amino group in the tail decreases the charge, which results in decreased potency; the analogous compounds with a methyl group at this position, such as **2e** and **2f**, show slightly better binding affinity to nNOS (Table 1). The methyl group should increase the basicity of the amino group in these two compounds compared to the cyclopropyl-containing counterparts. Although the tail amino groups in both the methyl and cyclopropyl inhibitors superimpose well, and both are in position to H-bond with Glu592 (Fig. 2), the higher basicity of the tail amino group ( $\text{p}K_a = 8.0$ , calculated by ACD/Labs 12.0), resulting from the methyl group compared to the cyclopropyl group, very likely contributes to the tighter binding of the methyl inhibitors. The higher affinity of **2e** over **2f** also is readily understood on the basis of amine-Glu592 interactions (Fig. 3). In **2f** the amino nitrogen is pointing away from the Glu592 side chain because of the *R*-chirality at the methyl position in this inhibitor. The *S*-stereochemistry seen in the nNOS-**2e** structure must be the dominant one preferred by the enzyme because it is the only enantiomer observed in the structure, even though **2e** used for the crystal soak is a racemic (*R/S*) mixture. This is consistent with the lower  $K_i$  value towards nNOS measured for **2e** versus **2f** (Table 1). The *R*-configuration can only be observed when the enantiomer pure compound (**2f**) is used.

To explore the structural basis for isoform selectivity of these cyclopropyl-containing inhibitors, crystal structures of eNOS with

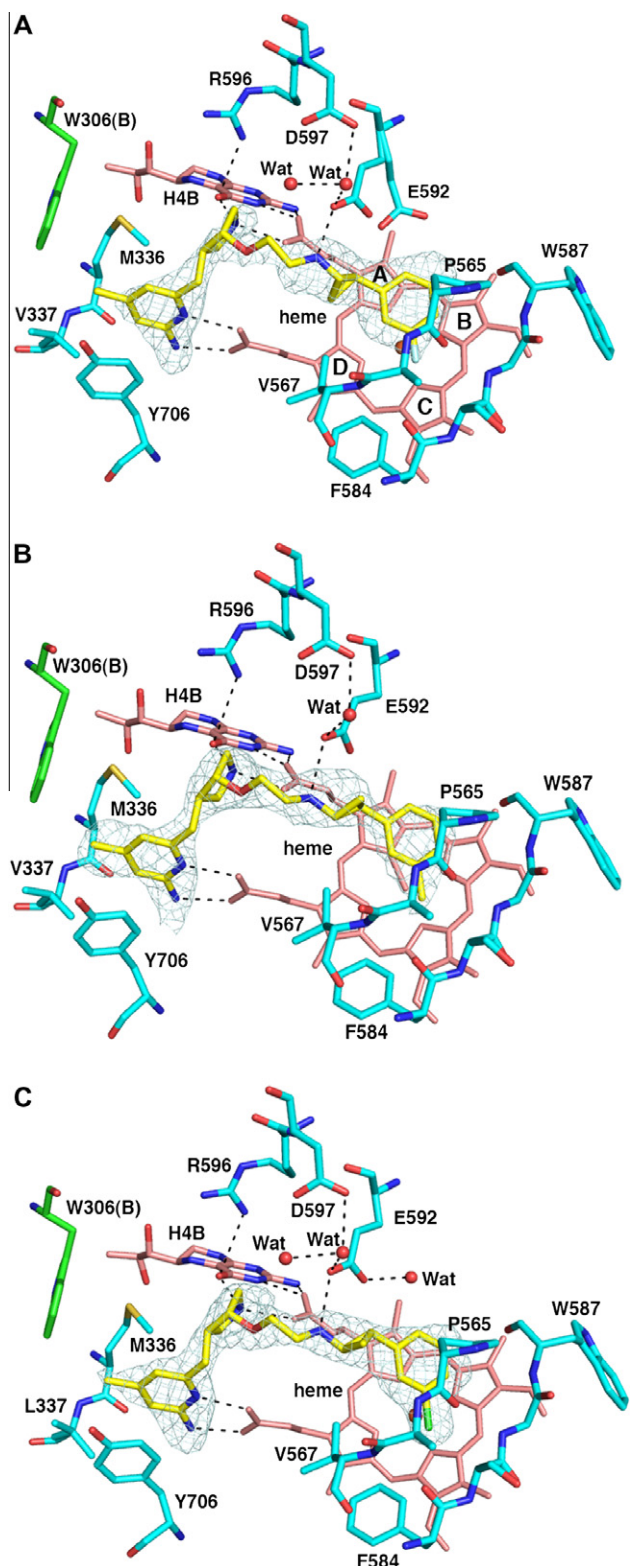


**Figure 1.** The nNOS active site structure with (A) **2b** (1.85 Å, PDB code 3RQJ), (B) **2c** (2.21 Å, 3RQK), or (C) **2d** (1.93 Å, 3RQL) bound. The omit  $F_o - F_c$  difference density contoured at  $3\sigma$  level is shown around the bound inhibitor. Note that the two alternate Glu592 side chain rotamers are observed for **2b**, but only the new rotamer is seen for **2c** and **2d**. Significant hydrogen bonds are depicted with dashed lines. The heme pyrrole ring positions are labeled in panel A. All structural figures were made with PyMol ([www.pymol.org](http://www.pymol.org)).

**2d** or **2e** bound were also determined as shown in Figure 4. Both inhibitors show the same binding mode in eNOS as that observed in nNOS structures (see Figs 1C and 3A). For eNOS-**2d** the bulky

chlorophenyl ring also forces the Glu363 side chain into its alternate rotamer conformation to avoid the potential clashes with Glu363 in its native rotamer conformation. For eNOS-**2e**, the smaller fluorophenyl ring and the absence of the cyclopropyl ring allow both Glu363 rotamer conformations to exist. In both cases, the enzyme-inhibitor interactions right above the heme in eNOS replicate what we have seen in nNOS. However, the binding affinity of these inhibitors to eNOS is significantly lower than that to nNOS. Isoform selection has been attributed primarily to two amino acid differences in the active site of NOS, Asp597 in nNOS versus Asn368 in eNOS and Met336 in nNOS versus Val106 in eNOS. Binding free energy calculations<sup>19</sup> indicated that although Asp597 (or Asn368) is not directly involved in binding of these pyrrolidine inhibitors, it does impose a significant electrostatic influence on how tight these inhibitors fit into the NOS active site. On the other side of the binding site, the Met336 (Val106) residue does contact the aminopyridine ring of the inhibitors. One of the valine methyl groups actually makes close contact with the inhibitor, thereby pushing the aminopyridine ring of inhibitor farther away from the Val106 position in eNOS compared to the aminopyridine position seen in nNOS. This different position of the aminopyridine ring in eNOS also pushes the Tyr477 side chain away relative to the Tyr706 position in nNOS, and as a result, Tyr706 in nNOS makes better stacking interactions with the aminopyridine ring of the inhibitor than does Tyr477 in eNOS. Taken together these differences observed between eNOS and nNOS provide a structural basis for the relatively poor binding of these inhibitors to eNOS.

In summary, the cyclopropyl containing pyrrolidine inhibitors reported in this study show a decrease in potency with both nNOS and eNOS compared with parental inhibitor **1**. This may result in part from the lowered basicity of the tail amino group. The structures here demonstrate the importance of the hydrogen bond strength of this amino group to the alternate side chain rotamer of the active site Glu residue. Weakening of this hydrogen bond results in a loss in potency toward nNOS, leading to poorer isoform selectivity of these more rigid cyclopropyl-containing inhibitors. These observations indicate that other chemical modifications are needed to retain the inhibitory potency in future inhibitor design.

## 4. Experimental section

### 4.1. General method A: Rh(II)-catalyzed cyclopropanation

To a solution of styrene derivative **4a–c** (20 mmol) in dry toluene (40 mL) was added  $\text{Rh}_2(\text{OAc})_4$  (0.4 mmol) catalyst. The resulting mixture was heated at 80 °C for 30 min, then ethyl diazoacetate (10 mmol) was added dropwise at the same temperature over a period of 1 h. The reaction mixture was allowed to stir at 85 °C for an additional 2 h and then cooled to room temperature. The solvent was removed by rotary evaporation, and the resulting oil was purified by flash chromatography (1–10% ethyl acetate in hexanes) to generate **5a–c** as mixtures of cis/trans isomers.

### 4.2. General method B: epimerization and hydrolysis

To a solution of **5a–c** (10 mmol) in EtOH (10 mL) was added  $\text{NaOCH}_3$  (40 mL) portionwise. The reaction solution was heated under reflux for 40 h and then concentrated by rotary evaporation. The resulting residue was partitioned between  $\text{CH}_2\text{Cl}_2$  (200 mL) and  $\text{H}_2\text{O}$  (100 mL). The aqueous layer was extracted with  $\text{CH}_2\text{Cl}_2$  ( $2 \times 100$  mL). The combined organic layers were dried over  $\text{Na}_2\text{SO}_4$  and concentrated. The crude ethyl ester was taken up in MeOH (70 mL), to which was added LiOH (345 mg, 15 mmol) and  $\text{H}_2\text{O}$

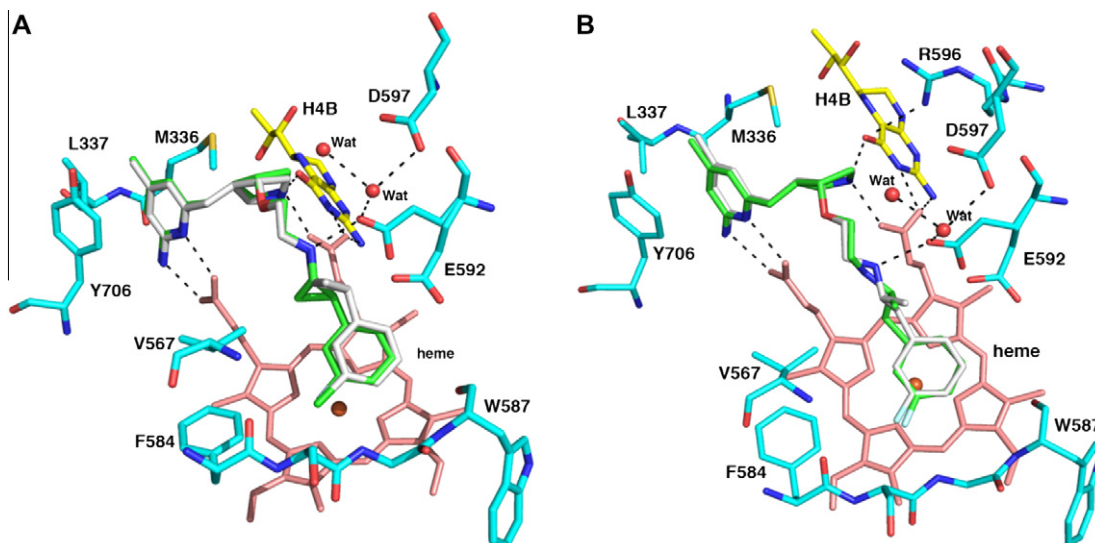


**Figure 2.** (A) The active site structure of nNOS-2b (green, 3RQJ) with the molecule of 2d (gray, 3RQL) overlaid in order to illustrate the chirality difference at the cyclopropyl ring. Two alternate Glu592 side chain rotamers are shown. (B) The active site structure of nNOS-2e (gray, 3RQM) with the molecule of 2f (green, 3RQN) overlaid. The two compounds in the structures show different stereochemistry (*S* or *R*) at the position of the methyl group.

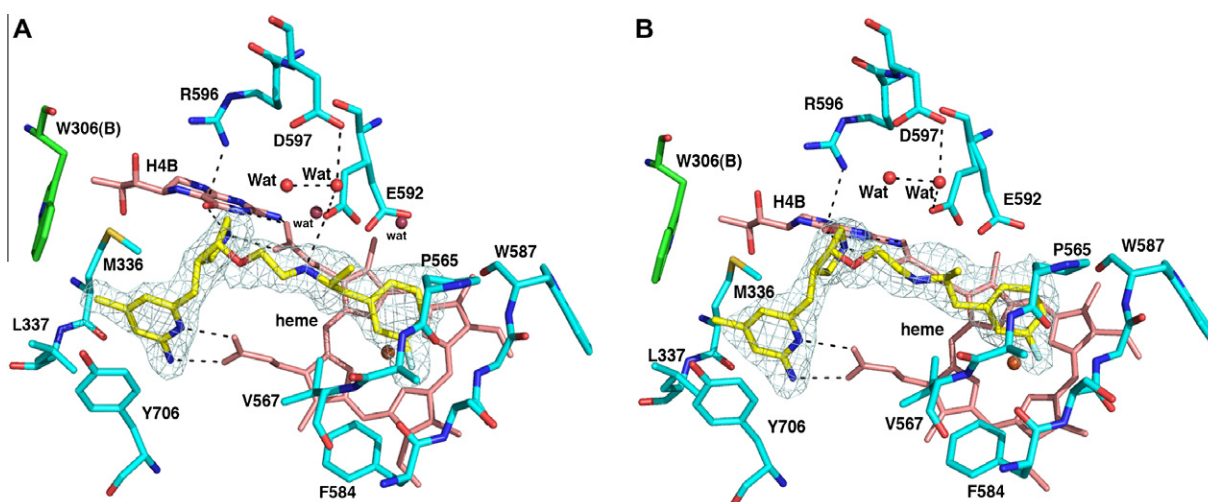


**Figure 3.** The active site of nNOS with (A) 2e (1.95 Å, 3RQM) or (B) 2f (1.95 Å, 3RQN) bound. The omit  $F_o - F_c$  difference density contoured at  $3\sigma$  level is shown around the bound inhibitor. Significant hydrogen bonds are depicted with dashed lines. In panel A, two partially occupied water molecules are also shown which are complementary to the two alternate Glu592 side chain positions.

(70 mL). The reaction was heated at 70 °C for 16 h. After cooling to room temperature, MeOH was removed by rotary evaporation. The resulting aqueous solution was acidified with concentrated HCl to pH 1 and then extracted with ethyl acetate ( $3 \times 150$  mL). The combined organic layers were dried over  $\text{Na}_2\text{SO}_4$ , and concentrated. The crude product was purified by flash chromatography to yield **6a–c** (75–80%) as white solids.

### 4.3. General method C: Curtius rearrangement

To a solution of **6a–c** (2.0 mmol) in dry *t*-BuOH (0.3 M) was added diphenyl phosphorazidate (DPPA, 2.2 mmol) and TEA (3.0 mmol). The reaction solution was heated at 85 °C for two days then cooled to room temperature and concentrated. The resulting solution was partitioned between ether (50 mL) and  $\text{NaHCO}_3$  (50 mL). The aqueous layer was extracted with ether ( $2 \times 50$  mL). The combined organic layers were dried over  $\text{Na}_2\text{SO}_4$  and

concentrated. The crude product was purified by flash chromatography to yield **7a–c** (75–82%) as white solids.

### 4.4. General method D: Boc-deprotection of 7a–c

To a solution of **7a–c** (1.0 mmol) in  $\text{CH}_2\text{Cl}_2$  (5 mL) was added TFA (5 mL). The reaction mixture was stirred at room temperature for 30 min. The solvent was removed by rotary evaporation. The yellow oil was dried under vacuum for 24 h to give crude amines **3a–c** as yellow oils, which were used in the next step without further purification.

### 4.5. General method E: reductive amination

To a solution of aldehyde (0.1 mmol) in  $\text{CH}_2\text{Cl}_2$  (3 mL) was added amine (0.11 mmol), followed by TEA (0.2 mmol), and  $\text{NaBH}(\text{OAc})_3$  (0.12 mmol). The mixture was stirred at room

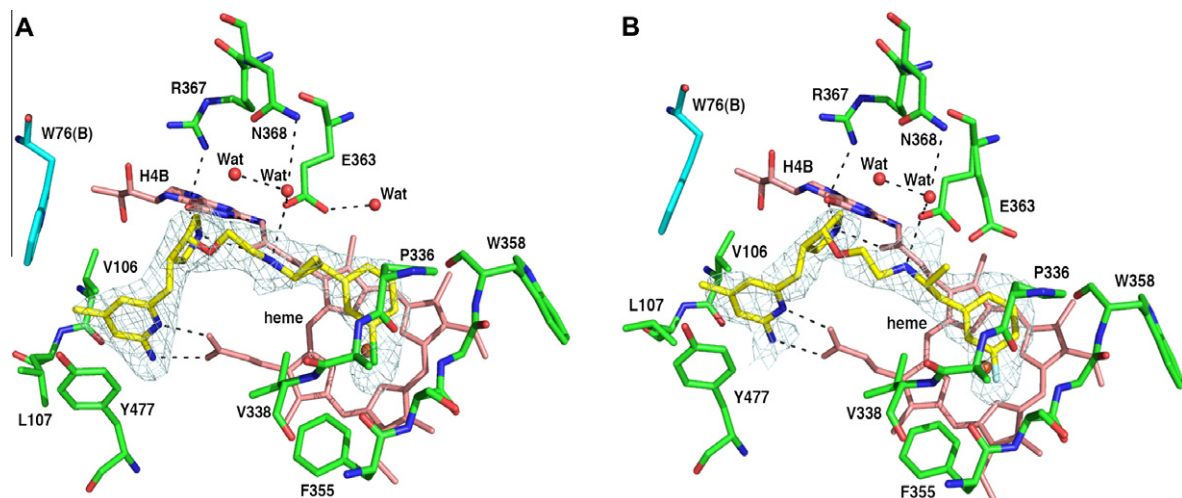


**Figure 4.** The eNOS active site with (A) **2d** (2.08 Å, 3RQO) or (B) **2e** (2.35 Å, 3RQP) bound. The omit  $F_o - F_c$  difference density contoured at  $3\sigma$  level is shown around the bound inhibitor. Significant hydrogen bonds are depicted with dashed lines.

temperature for an additional 3 h and then concentrated. The crude product was purified by flash column chromatography (ethyl acetate/hexanes, 2:1–4:1) to give the product as a colorless oil.

#### 4.6. General method F: Boc-deprotection of 10a–d and 11e–f

To a solution of tri-Boc-protected inhibitor (0.2 mmol) in MeOH (0.5 mL) was added 6 N HCl (1.0 mL). The reaction mixture was allowed to stand at room temperature for 16 h and then concentrated. The resulting pale yellow oil was evacuated for 30 h to give the inhibitors (95–99%).

#### 4.7. 2-(3-Fluorophenyl)cyclopropanecarboxylic acid (**6a**)

Compound **6a** was synthesized using general method A and B (75%):  $^1\text{H NMR}$  (500 MHz,  $\text{CDCl}_3$ )  $\delta$  0.87–0.91 (dd,  $J = 6.0, 13.5$  Hz, 1H), 1.21–1.29 (m, 1H), 1.39–1.43 (ddd,  $J = 5.0, 6.5, 8.0$  Hz, 1H), 1.67–1.72 (m, 1H), 1.90–1.94 (m, 1H), 2.58–2.63 (m, 1H), 6.79–6.82 (dd,  $J = 2.0, 5.5$  Hz, 1H), 6.90–6.95 (m, 2H), 7.24–7.28 (m, 1H), 8.90–11.00 (br s, 1H);  $^{13}\text{C NMR}$  (125 MHz,  $\text{CDCl}_3$ )  $\delta$  17.8, 24.4, 26.9, 31.8, 113.3, 113.5, 113.8, 114.0, 122.30, 122.32, 130.2, 130.3, 142.4, 142.5, 162.2, 164.2, 179.8; LCQ-MS ( $\text{M}-\text{H}^+$ ) calcd for  $\text{C}_{10}\text{H}_8\text{FO}_2$  179, found 179.

#### 4.8. 2-*m*-Tolylcyclopropanecarboxylic acid (**6b**)

Compound **6b** was synthesized using general method A and B (77%):  $^1\text{H NMR}$  (500 MHz,  $\text{CDCl}_3$ )  $\delta$  1.30–1.40 (ddd,  $J = 4.5, 7.0, 7.5$  Hz, 1H), 1.60–1.65 (dd,  $J = 5.0, 9.0$  Hz, 1H), 1.85–1.90 (ddd,  $J = 4.5, 5.0, 7.5$  Hz, 1H), 2.30 (s, 3H), 2.50–2.60 (ddd,  $J = 4.5, 7.0, 9.0$  Hz, 1H), 6.85–6.95 (m, 1H), 7.00–7.05 (m, 1H), 7.15–7.22 (m, 2H), 9.00–11.00 (br s, 1H);  $^{13}\text{C NMR}$  (125 MHz,  $\text{CDCl}_3$ )  $\delta$  17.5, 21.4, 24.0, 27.1, 123.2, 127.0, 127.4, 128.4, 138.2, 139.4, 180.1; LCQ-MS ( $\text{M}-\text{H}^+$ ) calcd for  $\text{C}_{11}\text{H}_{13}\text{O}_2$  177, found 177.

#### 4.9. 2-(3-Chlorophenyl)cyclopropanecarboxylic acid (**6c**)

Compound **6c** was synthesized using general method A and B (80%):  $^1\text{H NMR}$  (500 MHz,  $\text{CDCl}_3$ )  $\delta$  1.30–1.40 (ddd,  $J = 2.0, 3.5, 7.0$  Hz, 1H), 1.60–1.65 (dd,  $J = 5.0, 9.0$  Hz, 1H), 1.85–1.91 (m, 1H), 2.50–2.60 (m, 1H), 6.85–7.02 (m, 1H), 7.05–7.10 (m, 1H), 7.15–7.22 (m, 2H), 9.00–11.00 (br s, 1H);  $^{13}\text{C NMR}$  (125 MHz,  $\text{CDCl}_3$ )  $\delta$  17.8, 24.4, 26.9, 31.8, 113.3, 113.5, 113.8, 114.0, 122.30, 122.32,

130.2, 130.3, 142.4, 142.5, 162.2, 164.2, 179.8; LC-MS ( $\text{M}-\text{H}^+$ ) calcd for  $\text{C}_{10}\text{H}_{10}\text{ClO}_2$  197, found 197.

#### 4.10. *tert*-Butyl 2-(3-fluorophenyl)cyclopropylcarbamate (**7a**)

Compound **7a** was synthesized using general method C (75%):  $^1\text{H NMR}$  (500 MHz,  $\text{CDCl}_3$ )  $\delta$  1.10–1.25 (m, 1H), 1.40–1.55 (m, 10H), 2.00–2.10 (br s, 1H), 2.73 (br s, 1H), 5.04 (br s, 1H), 6.82–6.88 (m, 2H), 6.92–6.94 (d,  $J = 7.5$  Hz, 1H), 7.20–7.25 (dd,  $J = 7.5, 14.0$  Hz, 1H);  $^{13}\text{C NMR}$  (125 MHz,  $\text{CDCl}_3$ )  $\delta$  16.6, 25.1, 28.6, 32.9, 113.0, 113.2, 113.4, 113.6, 122.4, 129.9, 130.0, 130.1, 143.77, 143.83, 162.2, 164.1; LCQ-MS ( $\text{M}+\text{H}^+$ ) calcd for  $\text{C}_{14}\text{H}_{19}\text{FNO}_2$  252, found 252.

#### 4.11. *tert*-Butyl 2-*m*-tolylcyclopropylcarbamate (**7b**)

Compound **7b** was synthesized using general method C (82%):  $^1\text{H NMR}$  (500 MHz,  $\text{CDCl}_3$ )  $\delta$  1.00–1.20 (m, 1H), 1.46 (s, 9H), 1.95–2.05 (ddd,  $J = 3.0, 6.5, 9.5$  Hz, 1H), 2.31 (s, 3H), 2.74 (br s, 1H), 4.85 (br s, 1H), 6.91–6.93 (m, 2H), 6.97–6.99 (d,  $J = 7.5$  Hz, 1H), 7.13–7.16 (dd,  $J = 7.5, 8.0$  Hz, 1H);  $^{13}\text{C NMR}$  (125 MHz,  $\text{CDCl}_3$ )  $\delta$  16.3, 21.4, 24.5, 28.4, 32.6, 120.2, 120.3, 123.4, 126.1, 126.8, 127.2, 128.2, 130.1, 137.9, 140.6; LCQ-MS ( $\text{M}+\text{H}^+$ ) calcd for  $\text{C}_{15}\text{H}_{21}\text{NO}_2$  248, found 248.

#### 4.12. *tert*-Butyl 2-(3-chlorofluorophenyl)cyclopropylcarbamate (**7c**)

Compound **7c** was synthesized using general method C (77%):  $^1\text{H NMR}$  (500 MHz,  $\text{CDCl}_3$ )  $\delta$  1.14–1.17 (dd,  $J = 6.5, 7.0$  Hz, 2H), 1.45 (s, 9H), 1.99–2.03 (ddd,  $J = 2.5, 7.5, 10.5$  Hz, 1H), 2.72 (br s, 1H), 4.88 (br s, 1H), 6.95–7.02 (d,  $J = 7.0$  Hz, 1H), 7.10–7.25 (m, 3H);  $^{13}\text{C NMR}$  (125 MHz,  $\text{CDCl}_3$ )  $\delta$  16.3, 24.5, 28.4, 32.6, 120.1, 120.3, 124.8, 126.2, 126.6, 129.5, 129.9, 134.1, 142.9; LCQ-MS ( $\text{M}+\text{H}^+$ ) calcd for  $\text{C}_{14}\text{H}_{19}\text{ClNO}_2$  268, found 268.

#### 4.13. Compounds **8a** and **8b**

To a solution of amine **3a** (450 mg, 3.0 mmol) in  $\text{CH}_2\text{Cl}_2$  was added camphanic chloride (650 mg, 3.0 mmol) followed by TEA (510  $\mu\text{L}$ , 3.75 mmol). The reaction was allowed to stir at room temperature for 30 min and then concentrated. The resulting oil was purified by flash chromatography (ethyl acetate/hexanes, 1:4) to

generate **8a** (445 mg, 45%):  $^1\text{H}$  NMR (500 MHz,  $\text{CDCl}_3$ )  $\delta$  0.92 (s, 3H), 1.12 (s, 6H), 1.19–1.22 (m, 1H), 1.28–1.30 (m, 2H), 1.65–1.75 (m, 1H), 1.85–2.00 (m, 2H), 2.05–2.15 (m, 1H), 2.50–2.60 (m, 1H), 2.90–2.98 (m, 1H), 6.68 (br s, 1H), 6.84–6.90 (m, 2H), 6.95–6.97 (d,  $J=7.5$  Hz, 1H), 7.21–7.25 (m, 1H);  $^{13}\text{C}$  NMR (125 MHz,  $\text{CDCl}_3$ )  $\delta$  9.7, 15.8, 16.5, 16.7, 24.67, 24.78, 29.0, 30.3, 31.6, 54.0, 55.3, 92.4, 113.1, 113.27, 113.32, 113.5, 122.30, 122.32, 129.8, 129.9, 142.6, 142.7, 162.0, 163.9, 168.3, 178.2; LC-TOF ( $\text{M}+\text{H}^+$ ) calcd for  $\text{C}_{19}\text{H}_{23}\text{FNO}_3$  332.1662, found 332.1673.

Compound **8b** (360 mg, 36%):  $^1\text{H}$  NMR (500 MHz,  $\text{CDCl}_3$ )  $\delta$  0.91 (s, 3H), 1.11 (s, 6H), 1.20–1.35 (m, 3H), 1.65–1.75 (m, 1H), 1.85–2.00 (m, 2H), 2.00–2.10 (m, 1H), 2.50–2.58 (m, 1H), 2.89–2.95 (m, 1H), 6.67 (br s, 1H), 6.84–6.90 (m, 2H), 6.95–6.97 (d,  $J=8.0$  Hz, 1H), 7.21–7.24 (m, 1H);  $^{13}\text{C}$  NMR (125 MHz,  $\text{CDCl}_3$ )  $\delta$  9.7, 16.0, 16.5, 16.7, 24.61, 24.63, 29.0, 30.3, 31.5, 54.0, 55.3, 92.38, 92.40, 113.1, 113.29, 113.32, 113.4, 113.5, 113.6, 122.30, 122.32, 129.8, 129.9, 142.66, 142.72, 162.0, 163.9, 168.2, 168.3, 178.2; LC-TOF ( $\text{M}+\text{H}^+$ ) calcd for  $\text{C}_{19}\text{H}_{23}\text{FNO}_3$  332.1662, found 332.1677.

#### 4.14. (1S,2R)-2-(3-Fluorophenyl)cyclopropanamine (3d)

To a solution of **8a** (330 mg, 1.0 mmol) in EtOH (5 mL) was slowly added 12 N HCl (10 mL). The resulting mixture was heated under reflux for 72 h and then cooled to room temperature. The solvent was removed by rotary evaporation, and the resulting crude material was purified with flash chromatography (2–5% MeOH in  $\text{CH}_2\text{Cl}_2$ ) to give **3d** as a yellow oil (105 mg, 70%):  $^1\text{H}$  NMR (500 MHz,  $\text{CDCl}_3$ )  $\delta$  1.10–1.30 (br s, 1H), 1.40–1.60 (br s, 1H), 2.30–2.50 (br s, 1H), 2.70–2.90 (br s, 1H), 6.70–6.72 (m, 1H), 6.72–6.77 (m, 1H), 6.89–7.00 (m, 1H), 7.10–7.30 (m, 1H), 7.80–8.20 (br s, 2H);  $^{13}\text{C}$  NMR (125 MHz,  $\text{CDCl}_3$ )  $\delta$  13.2, 21.5, 31.6, 113.5, 113.7, 114.2, 114.4, 122.29, 122.31, 130.4, 130.5, 140.1, 140.2; LC-TOF ( $\text{M}+\text{H}^+$ ) calcd for  $\text{C}_9\text{H}_{11}\text{FN}$  152.0876, found 152.0870.

#### 4.15. (1R,2S)-2-(3-Fluorophenyl)cyclopropanamine (3e)

Compound **3e** was synthesized using a similar procedure to that of **3d** using **8b** as a starting material (67%):  $^1\text{H}$  NMR (500 MHz,  $\text{CDCl}_3$ )  $\delta$  1.10–1.30 (br s, 1H), 1.40–1.60 (br s, 1H), 2.30–2.50 (br s, 1H), 2.70–2.90 (br s, 1H), 6.70–6.72 (m, 1H), 6.72–6.77 (m, 1H), 6.89–7.00 (m, 1H), 7.10–7.30 (m, 1H), 7.80–8.20 (br s, 2H);  $^{13}\text{C}$  NMR (125 MHz,  $\text{CDCl}_3$ )  $\delta$  13.2, 21.5, 31.6, 113.5, 113.7, 114.2, 114.4, 122.29, 122.31, 130.4, 130.5, 140.1, 140.2; LC-TOF ( $\text{M}+\text{H}^+$ ) calcd for  $\text{C}_9\text{H}_{11}\text{FN}$  152.0876, found 152.0870.

#### 4.16. (3R,4R)-tert-Butyl 3-((6-(bis(tert-butoxycarbonyl)amino)-4-methylpyridin-2-yl)methyl)-4-(2-((1S,2R/1R,2S)-2-(3-fluorophenyl)cyclopropylamino)ethoxy)pyrrolidine-1-carboxylate (10a)

Compound **10a** was synthesized using general method D (81%):  $^1\text{H}$  NMR (500 MHz,  $\text{CDCl}_3$ )  $\delta$  0.95–1.00 (m, 1H), 1.06–1.10 (m, 1H), 1.40–1.46 (m, 27H), 1.86–1.90 (m, 1H), 2.26–2.33 (m, 3H), 2.35–2.40 (m, 1H), 2.60–2.75 (m, 1H), 2.76–2.85 (m, 1H), 2.86–2.92 (m, 2H), 2.95–2.98 (m, 1H), 3.05–3.13 (m, 1H), 3.24–3.30 (m, 1H), 3.30–3.35 (m, 1H), 3.36–3.51 (m, 1H), 3.57–3.75 (m, 1H), 3.77–3.85 (m, 1H), 6.85–6.92 (m, 2H), 6.93–7.20 (m, 4H);  $^{13}\text{C}$  NMR (100 MHz,  $\text{CDCl}_3$ )  $\delta$  17.4, 17.5, 17.6, 18.7, 20.9, 21.0, 22.2, 24.9, 25.0, 25.3, 26.2, 27.9, 28.5, 34.6, 34.7, 35.6, 41.3, 41.4, 41.5, 41.6, 42.5, 43.1, 48.7, 48.8, 49.1, 50.3, 52.0, 68.4, 68.5, 76.7, 78.6, 79.2, 79.3, 79.4, 82.8, 82.9, 119.5, 119.6, 122.7, 124.0, 124.07, 124.10, 124.12, 124.3, 125.5, 125.6, 125.7, 125.81, 125.83, 125.86, 125.94, 128.5, 128.6, 129.4, 129.5, 129.6, 132.0, 132.1, 134.1, 134.2, 143.6, 144.6, 144.7, 149.6, 151.47, 151.53, 151.8, 154.8,

159.7; LC-TOF ( $\text{M}+\text{H}^+$ ) calcd for  $\text{C}_{43}\text{H}_{60}\text{F}_3\text{N}_4\text{O}_8$  685.3977, found 685.3991.

#### 4.17. (3R,4R)-tert-Butyl 3-((6-(bis(tert-butoxycarbonyl)amino)-4-methylpyridin-2-yl)methyl)-4-(2-((1S,2R)-2-(3-fluorophenyl)cyclopropylamino)ethoxy)pyrrolidine-1-carboxylate (10b)

Compound **10b** was synthesized using general method D (82%):  $^1\text{H}$  NMR (500 MHz,  $\text{CDCl}_3$ )  $\delta$  0.95–1.01 (m, 1H), 1.10–1.15 (m, 1H), 1.40–1.45 (m, 27H), 1.89–1.92 (m, 1H), 2.28–2.32 (m, 3H), 2.33–2.37 (m, 1H), 2.60–2.75 (m, 1H), 2.76–2.83 (m, 1H), 2.85–2.93 (m, 2H), 2.95–3.00 (m, 1H), 3.05–3.15 (m, 1H), 3.27–3.31 (m, 1H), 3.32–3.34 (m, 1H), 3.35–3.55 (m, 1H), 3.57–3.74 (m, 1H), 3.75–3.85 (m, 1H), 6.65–6.72 (m, 1H), 6.80–6.89 (m, 2H), 6.90–6.95 (m, 2H), 7.15–7.20 (m, 1H);  $^{13}\text{C}$  NMR (100 MHz,  $\text{CDCl}_3$ )  $\delta$  14.2, 17.4, 17.5, 21.0, 22.7, 24.7, 24.8, 27.9, 28.5, 29.7, 31.6, 34.6, 34.7, 36.6, 41.4, 41.5, 42.5, 43.1, 44.7, 48.7, 48.8, 49.1, 50.3, 50.9, 60.4, 68.3, 78.6, 79.2, 79.3, 79.4, 82.8, 82.9, 112.2, 112.4, 112.6, 119.5, 119.6, 121.6, 122.7, 128.5, 128.6, 129.6, 129.7, 131.9, 132.0, 132.1, 132.2, 149.6, 151.5, 151.8, 154.6, 154.8, 159.0, 159.1, 162.0, 163.9; LC-TOF ( $\text{M}+\text{H}^+$ ) calcd for  $\text{C}_{37}\text{H}_{54}\text{FN}_4\text{O}_7$  685.3977, found 685.3979.

#### 4.18. (3R,4R)-tert-Butyl 3-((6-(bis(tert-butoxycarbonyl)amino)-4-methylpyridin-2-yl)methyl)-4-(2-((1S,2R/1R,2S)-2-m-tolylcyclopropylamino)ethoxy)pyrrolidine-1-carboxylate (10c)

Compound **10c** was synthesized using general method D (87%):  $^1\text{H}$  NMR (500 MHz,  $\text{CDCl}_3$ )  $\delta$  0.90–0.97 (m, 1H), 1.00–1.05 (m, 1H), 1.40–1.45 (m, 27H), 1.84–1.91 (m, 1H), 2.27–2.32 (m, 6H), 2.33–2.40 (m, 1H), 2.60–2.75 (m, 1H), 2.75–2.83 (m, 1H), 2.85–2.93 (m, 2H), 2.95–3.00 (m, 1H), 3.05–3.15 (m, 1H), 3.25–3.30 (m, 1H), 3.31–3.34 (m, 1H), 3.35–3.55 (m, 1H), 3.57–3.74 (m, 1H), 3.75–3.85 (m, 1H), 6.85–6.95 (m, 4H), 6.92–7.01 (m, 2H), 7.10–7.20 (m, 2H);  $^{13}\text{C}$  NMR (100 MHz,  $\text{CDCl}_3$ )  $\delta$  13.7, 14.1, 14.2, 17.2, 17.3, 17.4, 19.1, 20.9, 21.0, 21.1, 21.4, 22.2, 24.96, 24.99, 25.0, 25.5, 27.9, 28.5, 29.7, 30.6, 34.6, 34.7, 41.0, 41.1, 42.6, 43.2, 48.8, 48.9, 49.0, 49.1, 50.3, 60.4, 64.4, 68.4, 78.6, 79.2, 79.3, 79.4, 82.8, 82.9, 119.5, 119.6, 122.7, 122.8, 122.9, 126.3, 126.5, 126.6, 126.7, 126.8, 128.17, 128.24, 128.3, 128.5, 128.6, 132.0, 132.1, 137.8, 137.9, 141.3, 142.3, 149.6, 151.4, 151.5, 151.8, 154.8, 159.1, 159.2, 171.2; LC-TOF ( $\text{M}+\text{H}^+$ ) calcd for  $\text{C}_{38}\text{H}_{57}\text{N}_4\text{O}_7$  681.4227, found 681.4224.

#### 4.19. (3R,4R)-tert-Butyl 3-((6-(bis(tert-butoxycarbonyl)amino)-4-methylpyridin-2-yl)methyl)-4-(2-((1S,2R/1R,2S)-2-(3-chlorophenyl)cyclopropylamino)ethoxy)pyrrolidine-1-carboxylate (10d)

Compound **10d** was synthesized using general method D (87%):  $^1\text{H}$  NMR (500 MHz,  $\text{CDCl}_3$ )  $\delta$  0.92–0.99 (m, 1H), 1.07–1.11 (m, 1H), 1.40–1.45 (m, 27H), 1.85–1.90 (m, 1H), 2.29–2.33 (m, 3H), 2.34–2.38 (m, 1H), 2.60–2.75 (m, 1H), 2.76–2.83 (m, 1H), 2.85–2.93 (m, 2H), 2.95–3.00 (m, 1H), 3.05–3.15 (m, 1H), 3.25–3.30 (m, 1H), 3.31–3.34 (m, 1H), 3.35–3.52 (m, 1H), 3.57–3.74 (m, 1H), 3.75–3.85 (m, 1H), 6.85–6.92 (m, 2H), 6.93–7.05 (m, 2H), 7.08–7.20 (m, 4H);  $^{13}\text{C}$  NMR (100 MHz,  $\text{CDCl}_3$ )  $\delta$  17.4, 17.5, 17.6, 18.7, 20.9, 21.0, 22.2, 24.9, 25.0, 25.3, 26.2, 27.9, 28.5, 34.6, 34.7, 35.6, 41.3, 41.4, 41.5, 41.6, 42.5, 43.1, 48.7, 48.8, 49.1, 50.3, 52.0, 68.4, 68.5, 76.7, 78.6, 79.2, 79.3, 79.4, 82.8, 82.9, 119.5, 119.6, 122.7, 124.0, 124.07, 124.10, 124.12, 124.3, 125.5, 125.6, 125.7, 125.81, 125.83, 125.86, 125.94, 128.5, 128.6, 129.4, 129.5, 129.6, 132.0, 132.1, 134.1, 134.2, 143.6, 144.6, 144.7, 149.6, 151.47, 151.53, 151.8, 154.8, 159.7; LC-TOF ( $\text{M}+\text{H}^+$ ) calcd for  $\text{C}_{37}\text{H}_{53}\text{ClN}_4\text{O}_7$  701.3681, found 701.3884.

**4.20. 6-(((3*R*,4*R*)-4-(2-((1*S*,2*R*/1*R*,2*S*)-2-(3-Fluorophenyl)-cyclopropylamino)ethoxy)pyrrolidin-3-yl)methyl)-4-methylpyridin-2-amine (2a)**

Compound **2a** was synthesized using general method E as a mixture of two diastereomers (99%): <sup>1</sup>H NMR (500 MHz, D<sub>2</sub>O) δ 1.30–1.40 (m, 1H), 1.41–1.48 (m, 1H), 2.10–2.20 (m, 3H), 2.30–2.50 (m, 1H), 2.51–2.77 (m, 2H), 2.80–2.90 (m, 1H), 2.91–3.03 (m, 1H), 3.04–3.40 (m, 3H), 3.41–3.72 (m, 2H), 3.73–3.88 (m, 1H), 3.90–4.11 (m, 1H), 4.40–4.50 (m, 1H), 6.30–6.60 (m, 2H), 6.70–6.90 (m, 2H), 7.00–7.20 (m, 2H); <sup>13</sup>C NMR (125 MHz, D<sub>2</sub>O) δ 12.6, 12.9, 20.7, 20.9, 21.2, 21.4, 29.1, 37.7, 37.8, 38.6, 41.5, 45.3, 47.3, 47.6, 47.7, 49.6, 63.8, 64.5, 78.3, 78.5, 109.0, 110.5, 113.2, 113.4, 113.8, 114.0, 114.3, 122.4, 127.2, 128.1, 129.2, 130.1, 136.4, 140.7, 140.9, 145.9, 146.6, 153.0, 154.0, 158.3, 161.8, 163.8; LC-TOF (M+H<sup>+</sup>) calcd for C<sub>21</sub>H<sub>30</sub>FN<sub>4</sub>O<sub>2</sub> 385.2404, found 385.2393.

**4.21. 6-(((3*R*,4*R*)-4-(2-((1*S*,2*R*)-2-(3-Fluorophenyl)-cyclopropylamino)ethoxy)pyrrolidin-3-yl)methyl)-4-methylpyridin-2-amine (2b)**

Compound **2b** was synthesized using general method E (95%): <sup>1</sup>H NMR (500 MHz, D<sub>2</sub>O) δ 1.30–1.40 (m, 1H), 1.41–1.46 (m, 1H), 2.18 (s, 3H), 2.19–2.20 (m, 1H), 2.40–2.50 (m, 1H), 2.55–2.70 (m, 2H), 2.81–3.00 (m, 3H), 3.19–3.23 (dd, *J* = 3.5, 13.5 Hz, 1H), 3.30–3.40 (m, 2H), 3.49–3.52 (m, 1H), 3.55–3.61 (m, 1H), 3.75–3.85 (m, 1H), 4.06 (br s, 1H), 6.38 (s, 1H), 6.54 (s, 1H), 6.80–6.95 (m, 3H), 7.15–7.25 (dd, *J* = 5.5, 10.5 Hz, 1H); <sup>13</sup>C NMR (125 MHz, D<sub>2</sub>O) δ 12.6, 20.4, 21.0, 28.8, 30.1, 38.4, 41.3, 47.1, 47.5, 49.3, 64.3, 78.3, 110.3, 112.9, 113.1, 113.6, 113.8, 114.0, 122.1, 128.9, 129.0, 130.4, 130.5, 131.8, 131.9, 133.1, 140.6, 140.7, 145.6, 153.9, 158.1; LC-TOF (M+H<sup>+</sup>) calcd for C<sub>21</sub>H<sub>30</sub>FN<sub>4</sub>O<sub>2</sub> 385.2404, found 385.2384.

**4.22. 4-Methyl-6-(((3*R*,4*R*)-4-(2-((1*S*,2*R*/1*R*,2*S*)-2-*m*-tolylcyclopropylamino)ethoxy)pyrrolidin-3-yl)methyl)pyridin-2-amine (2c)**

Inhibitor **2c** was synthesized using general method E as a mixture of two diastereomers (90%): <sup>1</sup>H NMR (500 MHz, D<sub>2</sub>O) δ 1.10–1.30 (m, 1H), 1.35–1.45 (m, 1H), 2.10–2.15 (m, 3H), 2.15–2.20 (m, 3H), 2.20–2.50 (m, 1H), 2.50–2.80 (m, 2H), 2.81–3.00 (m, 2H), 3.19–3.25 (m, 1H), 3.30–3.40 (m, 2H), 3.47–3.52 (m, 1H), 3.55–3.70 (m, 1H), 3.71–3.85 (m, 1H), 4.00–4.15 (m, 1H), 6.35–6.60 (m, 2H), 6.85–6.90 (m, 2H), 6.91–7.15 (m, 2H); <sup>13</sup>C NMR (125 MHz, D<sub>2</sub>O) δ 12.2, 12.3, 15.1, 20.2, 20.4, 20.5, 20.6, 20.7, 21.0, 21.6, 23.2, 28.8, 28.9, 30.1, 30.5, 31.8, 37.4, 38.5, 41.2, 41.3, 47.0, 47.2, 47.5, 49.2, 49.3, 63.6, 64.5, 78.1, 78.3, 110.2, 110.3, 113.9, 114.0, 122.9, 123.1, 123.3, 126.3, 126.5, 126.6, 126.7, 126.8, 127.5, 127.6, 127.7, 128.6, 128.7, 128.78, 128.82, 128.9, 129.0, 131.8, 131.9, 137.9, 138.1, 138.7, 138.9, 139.0, 145.59, 145.62, 153.8, 158.1; LC-TOF (M+H<sup>+</sup>) calcd for C<sub>21</sub>H<sub>30</sub>FN<sub>4</sub>O<sub>2</sub> 381.2654, found 381.2653.

**4.23. 6-(((3*R*,4*R*)-4-(2-((1*S*,2*R*/1*R*,2*S*)-2-(3-Chlorophenyl)-cyclopropylamino)ethoxy)pyrrolidin-3-yl)methyl)-4-methylpyridin-2-amine (2d)**

Compound **2d** was synthesized using general method E as a mixture of two diastereomers (91%): <sup>1</sup>H NMR (500 MHz, D<sub>2</sub>O) δ 1.10–1.30 (m, 1H), 1.35–1.50 (m, 1H), 2.15–2.20 (m, 3H), 2.25–2.30 (m, 1H), 2.35–2.50 (m, 1H), 2.55–2.70 (m, 2H), 2.70–2.77 (m, 1H), 2.81–3.00 (m, 2H), 3.19–3.25 (m, 1H), 3.30–3.40 (m, 1H), 3.49–3.52 (m, 1H), 3.55–3.70 (m, 1H), 3.75–3.85 (m, 1H), 4.05 (br

s, 0.5H), 4.12 (br s, 0.5H), 6.34 (s, 0.5H), 6.39 (s, 0.5H), 6.51 (s, 0.5H), 6.53 (s, 0.5H), 6.95–7.01 (m, 1H), 7.05–7.20 (m, 3H); <sup>13</sup>C NMR (125 MHz, D<sub>2</sub>O) δ 12.3, 12.4, 12.6, 20.3, 20.4, 20.5, 21.1, 28.8, 28.9, 30.6, 37.4, 38.6, 41.2, 41.3, 47.0, 47.1, 47.2, 47.5, 49.2, 49.3, 63.5, 64.5, 78.2, 78.4, 110.31, 110.34, 113.9, 114.0, 124.7, 124.75, 124.82, 126.1, 126.16, 126.23, 126.7, 126.9, 127.0, 130.0, 130.1, 130.2, 133.8, 133.9, 134.0, 140.2, 140.7, 145.52, 145.54, 153.8, 158.1; LC-TOF (M+H<sup>+</sup>) calcd for C<sub>22</sub>H<sub>30</sub>ClN<sub>4</sub>O 401.2108, found 401.2093.

**4.24. (3*R*,4*R*)-*tert*-Butyl 3-((6-(benzyl(*tert*-butoxycarbonyl)-amino)-4-methylpyridin-2-yl)methyl)-4-(2-((*tert*-butoxycarbonyl)((1*S*,2*R*/1*R*,2*S*)-2-(3-fluorophenyl)cyclopropyl)amino)ethoxy)-pyrrolidine-1-carboxylate (10e)**

To a solution of aldehyde **9b** (100 mg, 0.18 mmol) in CH<sub>2</sub>Cl<sub>2</sub> (2 mL) was added **3a** (60 mg, 0.37 mmol) followed by TEA (125 μL, 0.9 mmol). The mixture was allowed to stir at room temperature for 5 min before NaBH(OAc)<sub>3</sub> (50 mg, 0.23 mmol) was added. The reaction mixture was stirred for an additional 3 h then was partitioned between ethyl acetate (50 mL) and brine (25 mL). The organic layer was dried over Na<sub>2</sub>SO<sub>4</sub> and concentrated to yield crude secondary amine. To a solution of the resulting crude amine in MeOH (1.5 mL) was added (Boc)<sub>2</sub>O (120 mg, 0.56 mmol) and Et<sub>3</sub>N (75 μL, 0.56 mmol). The reaction mixture was stirred at room temp for 6 h and was partitioned between ethyl acetate (50 mL) and brine (20 mL). The organic layer was dried over Na<sub>2</sub>SO<sub>4</sub> and the solvents were removed by rotary evaporation. The resulting material was purified by flash column chromatography (ethyl acetate/hexanes, 1:4–1:2) to yield **10e** (70 mg, 60%) as a colorless oil (71%): <sup>1</sup>H NMR (500 MHz, CDCl<sub>3</sub>) δ 1.15–1.21 (m, 2H), 1.35–1.50 (m, 28H), 1.65–1.80 (br s, 1H), 2.10–2.20 (br s, 1H), 2.25–2.33 (m, 3H), 2.50–2.80 (m, 3H), 2.80–2.97 (m, 1H), 3.00–3.10 (m, 1H), 3.15–3.20 (m, 1H), 3.25–3.50 (m, 3H), 3.55–3.70 (m, 3H), 4.05–4.10 (m, 1H), 5.18 (s, 2H), 6.55–6.65 (m, 1H), 6.70–6.90 (m, 3H), 7.10–7.30 (m, 6H), 7.40–7.45 (m, 1H); <sup>13</sup>C NMR (125 MHz, CDCl<sub>3</sub>) δ 14.1, 14.3, 14.5, 19.5, 21.2, 21.4, 23.0, 28.5, 28.6, 28.9, 30.0, 30.7, 31.7, 34.7, 34.7, 40.2, 40.3, 42.9, 49.1, 49.6, 50.3, 50.4, 51.1, 60.6, 64.6, 78.1, 79.4, 79.7, 80.2, 81.3, 81.5, 112.9, 113.0, 117.2, 117.3, 120.2, 122.2, 126.7, 127.0, 127.2, 127.3, 128.3, 130.1, 140.2, 148.8, 148.8, 154.2, 154.7, 154.7, 155.1, 157.9, 162.1, 164.2, 171.4; LC-TOF (M+H<sup>+</sup>) calcd for C<sub>44</sub>H<sub>60</sub>FN<sub>4</sub>O<sub>7</sub> 775.4441, found 775.4432.

**4.25. (3*R*,4*R*)-*tert*-Butyl 3-((6-(benzyl(*tert*-butoxycarbonyl)-amino)-4-methylpyridin-2-yl)methyl)-4-(2-((*tert*-butoxycarbonyl)((1*S*,2*R*)-2-(3-fluorophenyl)cyclopropyl)amino)ethoxy)pyrrolidine-1-carboxylate (10f)**

Compound **10f** was synthesized, using a procedure similar to that for **10e** (60%), as a colorless oil (71%): <sup>1</sup>H NMR (500 MHz, CDCl<sub>3</sub>) δ 1.10–1.22 (m, 2H), 1.35–1.50 (m, 28H), 1.65–1.80 (br s, 1H), 2.10–2.20 (br s, 1H), 2.20–2.35 (m, 3H), 2.40–2.80 (m, 3H), 2.80–2.95 (m, 1H), 2.97–3.10 (m, 1H), 3.16–3.21 (m, 1H), 3.22–3.44 (m, 3H), 3.45–3.70 (m, 3H), 4.04–4.10 (m, 1H), 5.10–5.25 (br s, 2H), 6.55–6.65 (m, 1H), 6.65–6.95 (m, 3H), 7.10–7.27 (m, 6H), 7.31–7.45 (m, 1H); <sup>13</sup>C NMR (125 MHz, CDCl<sub>3</sub>) δ 14.0, 14.4, 14.5, 19.4, 21.3, 21.4, 22.9, 28.4, 28.7, 28.8, 30.0, 30.9, 31.8, 34.8, 34.9, 40.0, 40.1, 42.9, 49.1, 49.5, 50.2, 50.5, 51.1, 60.7, 64.6, 78.2, 79.4, 79.7, 80.2, 81.4, 81.5, 112.9, 113.0, 117.2, 117.3, 120.2, 122.1, 126.8, 127.1, 127.2, 127.3, 128.3, 130.0, 140.1, 148.7, 148.8, 154.1, 154.6, 154.7, 155.0, 157.9, 162.2, 164.1, 171.4, 171.5; LC-TOF (M+H<sup>+</sup>) calcd for C<sub>44</sub>H<sub>60</sub>FN<sub>4</sub>O<sub>7</sub> 775.4441, found 775.4441.

**4.26. 6-(((3R,4R)-4-(2-(((R/S)-1-(3-Fluorophenyl)propan-2-yl)amino)ethoxy)pyrrolidin-3-yl)methyl)-4-methylpyridin-2-amine (2e)**

To a solution of **10e** (0.2 mmol) in EtOH (20 mL) was added Pd(OH)<sub>2</sub>/C (100 mg). The reaction vessel was charged with H<sub>2</sub>, heated at 60 °C for 30 h, then cooled to room temperature. The catalyst was removed by filtration, and the resulting solution was concentrated by rotary evaporation. The crude material was purified by flash column chromatography (ethyl acetate/hexanes, 1:4–1:2) to yield **11e** as a white foamy solid. To a solution of the resulting **11e** in MeOH (0.5 mL) was added 6 N HCl (1.0 mL). The reaction mixture was allowed to stand at room temperature for 16 h. The solvent was removed by rotary evaporation. The crude product was recrystallized using cold diethyl ether to provide **2e** as a pale yellow solid (20 mg, 25%): <sup>1</sup>H NMR (500 MHz, D<sub>2</sub>O) δ 1.18–1.20 (m, 3H), 2.20 (s, 3H), 2.60–2.72 (m, 2H), 2.75–2.90 (m, 2H), 3.00–3.10 (m, 2H), 3.15–3.33 (m, 3H), 3.34–3.42 (m, 1H), 3.44–3.60 (m, 3H), 3.70–3.80 (m, 1H), 4.09 (s, 1H), 6.46–4.67 (m, 1H), 6.56 (s, 1H), 6.90–7.10 (m, 3H), 7.20–7.25 (m, 1H); <sup>13</sup>C NMR (125 MHz, D<sub>2</sub>O) δ 15.2, 15.5, 21.3, 29.2, 38.4, 38.5, 41.6, 41.7,

44.2, 44.4, 47.3, 49.5, 55.6, 64.0, 64.4, 78.4, 110.6, 114.3, 114.4, 114.5, 116.2, 116.4, 125.4, 125.6, 130.8, 130.9, 138.3, 145.9, 146.0, 154.1, 158.4, 161.9, 163.9; LC-TOF (M+H<sup>+</sup>) calcd for C<sub>22</sub>H<sub>32</sub>FN<sub>4</sub>O 387.2560, found 385.2556.

**4.27. 6-(((3R,4R)-4-(2-(((S)-1-(3-Fluorophenyl)propan-2-yl)amino)ethoxy)pyrrolidin-3-yl)methyl)-4-methylpyridin-2-amine (2f)**

Compound **2f** was synthesized using a procedure similar to that for **2e** (25%): <sup>1</sup>H NMR (500 MHz, D<sub>2</sub>O) δ 1.28–1.30 (d, J = 6.5 Hz, 3H), 2.31 (s, 3H), 2.75–2.85 (m, 2H), 2.85–3.00 (m, 2H), 3.10–3.20 (m, 2H), 3.30–3.37 (m, 2H), 3.37–3.46 (m, 1H), 3.46–3.55 (m, 1H), 3.55–3.70 (m, 3H), 3.80–3.90 (m, 1H), 4.20 (s, 1H), 6.57 (s, 1H), 6.67 (s, 1H), 7.00–7.05 (m, 1H), 7.06–7.09 (m, 1H), 7.09–7.13 (d, J = 7.5 Hz, 1H), 7.33–7.40 (dd, J = 7.5, 14.5 Hz, 1H); <sup>13</sup>C NMR (125 MHz, D<sub>2</sub>O) δ 15.0, 21.0, 29.0, 38.2, 41.4, 43.9, 47.0, 49.3, 55.4, 64.2, 78.1, 110.4, 114.0, 114.1, 114.3, 115.9, 116.1, 125.18, 125.20, 130.6, 130.7, 130.07, 130.13, 145.7, 153.9, 158.1, 161.7, 163.6; LC-TOF (M+H<sup>+</sup>) calcd for C<sub>22</sub>H<sub>32</sub>FN<sub>4</sub>O 387.2560, found 385.2547.

**Table 2**  
Crystallographic data collection and refinement statistics

Data set	nNOS-2b	nNOS-2c	nNOS-2d	nNOS-2e
<i>Data collection</i>				
PDB code	3RQJ	3RQK	3RQL	3RQM
Space group	P2 <sub>1</sub> 2 <sub>1</sub> 2 <sub>1</sub>			
Cell dimensions				
<i>a</i> , <i>b</i> , <i>c</i> (Å)	51.8, 110.7, 164.3	52.0, 111.5, 164.4	51.7, 110.8, 163.9	51.9, 110.4, 164.0
Resolution (Å)	1.85 (1.88–1.85)	2.20 (2.24–2.20)	1.93 (1.96–1.93)	1.95 (1.98–1.95)
<i>R</i> <sub>sym</sub> or <i>R</i> <sub>merge</sub>	0.044 (0.63)	0.076 (0.54)	0.052 (0.59)	0.061 (0.59)
<i>I</i> / <i>σ</i>	36.2 (2.5)	25.6 (2.1)	29.8 (2.3)	22.9 (2.0)
No. unique reflections	82,378	47,658	71,869	69,867
Completeness (%)	99.6 (99.7)	97.9 (97.5)	99.7 (100.0)	99.7 (99.5)
Redundancy	4.1 (4.1)	3.8 (3.7)	4.1 (4.0)	3.8 (3.6)
<i>Refinement</i>				
Resolution (Å)	1.85	2.21	1.93	1.95
No. reflections used	78,043	45,045	68,065	66,358
<i>R</i> <sub>work</sub> / <i>R</i> <sub>free</sub>	0.189/0.221	0.200/0.258	0.190/0.235	0.173/0.208
<i>No. atoms</i>				
Protein	6,677	6,662	6,697	6,672
Ligand/ion	185	185	188	179
Water	328	170	312	538
<i>R.m.s. deviations</i>				
Bond lengths (Å)	0.015	0.015	0.017	0.013
Bond angles (°)	1.508	1.535	1.637	1.372
Data set <sup>a</sup>	nNOS-2f		eNOS-2d	eNOS-2e
<i>Data collection</i>				
PDB code	3RQN		3RQO	3RQP
Space group	P2 <sub>1</sub> 2 <sub>1</sub> 2 <sub>1</sub>		P2 <sub>1</sub> 2 <sub>1</sub> 2 <sub>1</sub>	P2 <sub>1</sub> 2 <sub>1</sub> 2 <sub>1</sub>
Cell dimensions				
<i>a</i> , <i>b</i> , <i>c</i> (Å)	52.1, 110.9, 164.2		58.1, 106.6, 156.5	57.9, 106.6, 156.9
Resolution (Å)	1.95 (1.98–1.95)		2.08 (2.12–2.08)	2.35 (2.39–2.35)
<i>R</i> <sub>sym</sub> or <i>R</i> <sub>merge</sub>	0.056 (0.55)		0.072 (0.66)	0.086 (0.67)
<i>I</i> / <i>σ</i>	27.0 (2.6)		22.8 (2.1)	13.8 (1.5)
No. unique reflections	70,044		59,039	41,301
Completeness (%)	99.9 (100.0)		99.6 (99.9)	99.5 (99.2)
Redundancy	4.1 (4.1)		3.7 (3.8)	3.6 (3.5)
<i>Refinement</i>				
Resolution (Å)	1.95		2.08	2.35
No. reflections used	66,498		55,805	39,184
<i>R</i> <sub>work</sub> / <i>R</i> <sub>free</sub> <sup>b</sup>	0.173/0.209		0.174/0.221	0.178/0.228
<i>No. atoms</i>				
Protein	6,698		6,416	6,462
Ligand/ion	185		193	203
Water	396		403	255
<i>R.m.s. deviations</i>				
Bond lengths (Å)	0.013		0.015	0.014
Bond angles (°)	1.352		1.557	1.522

<sup>a</sup> See Table 1 for nomenclature and chemical formula of inhibitors.

<sup>b</sup> *R*<sub>free</sub> was calculated with the 5% of reflections set aside throughout the refinement. For each NOS isoform the set of reflections for the *R*<sub>free</sub> calculation were kept the same for all data sets according to those used in the data of the starting model.

## 5. Inhibitory activity assay

The three isozymes, murine macrophage iNOS, rat nNOS, and bovine eNOS, were recombinant enzymes, overexpressed in *Escherichia coli* and isolated as reported.<sup>30</sup> IC<sub>50</sub> values for inhibitors **2a–f** were measured for the three different isoforms of NOS using L-arginine as a substrate. The formation of nitric oxide was measured using a hemoglobin capture assay described previously.<sup>31</sup> All NOS isozymes were assayed at room temperature in a 100 mM Hepes buffer (pH 7.4) containing 10 μM L-arginine, 1.6 mM CaCl<sub>2</sub>, 11.6 μg/mL calmodulin, 100 μM DTT, 100 μM NADPH, 6.5 μM H<sub>4</sub>B, 3.0 μM oxyhemoglobin (for iNOS assays, no Ca<sup>2+</sup> and calmodulin were added). The assay was initiated by the addition of enzyme, and the initial rates of the enzymatic reactions were determined by monitoring the formation of NO–hemoglobin complex at 401 nm for 60 s. The corresponding K<sub>i</sub> values of inhibitors were calculated from the IC<sub>50</sub> values using Equation 1 with known K<sub>m</sub> values (rat nNOS, 1.3 μM; iNOS, 8.3 μM; eNOS, 1.7 μM).

$$K_i = IC_{50} / (1 + [S]/K_m) \quad (1)$$

## 6. Crystal structure determination

The preparation of protein samples of nNOS and eNOS heme domain and the procedures for crystal growth and inhibitor soaks were the same as reported.<sup>19</sup> The cryogenic (100 K) X-ray diffraction data were collected remotely at various beamlines at Stanford Synchrotron Radiation Light Source (SSRL) through the data collection control software Blu-Ice<sup>32</sup> and crystal mounting robot.

Raw data frames were indexed, integrated, and scaled using HKL2000.<sup>33</sup> The reflection files were then converted to the mtz format using routines Scalepack2mtz and Truncate in the CCP4 suite.<sup>34</sup> The binding of each inhibitor was revealed by the initial difference Fourier maps calculated with REFMAC.<sup>35</sup> The inhibitor molecules were then modeled in COOT<sup>36</sup> and refined using REFMAC. Water molecules were added in REFMAC and inspected visually through COOT. The TLS<sup>37</sup> protocol was implemented in the final stage of refinements with each subunit as one TLS group. The omit F<sub>o</sub> – F<sub>c</sub> electron density map was calculated at the end of the refinement with the coefficient DELFTW in a mtz file generated by a round of TLS refinement fed with an inhibitor-free coordinate file. The refined structures were validated in COOT before deposition in the RCSB protein data bank. The crystallographic data collection and structure refinement statistics are summarized in Table 2 with PDB accession codes included.

## Acknowledgments

The authors are grateful for financial support from the National Institutes of Health (GM49725 to RBS and GM57353 to TLP). We thank Dr. Bettie Sue Siler Masters (NIH Grant GM52419, with whose laboratory P.M. and L.J.R. are affiliated). B.S.S.M. also is grateful to the Welch Foundation for a Robert A. Welch Distinguished Professorship in Chemistry (AQ0012). P.M. is supported by Grant 0021620849 from MSMT of the Czech Republic. We also

thank the staff at SSRL for their assistance during the remote X-ray diffraction data collections.

## References and notes

- Alderton, W. K.; Cooper, C. E.; Knowles, R. G. *Biochem. J.* **2001**, *357*, 593.
- Marletta, M. A. *J. Biol. Chem.* **1993**, *268*, 12231.
- Marletta, M. A. *Cell* **1994**, *78*, 927.
- Hall, A. V.; Antoniou, H.; Wang, Y.; Cheung, A. H.; Arbus, A. M.; Olson, S. L.; Lu, W. C.; Kau, C. L.; Marsden, P. A. *J. Biol. Chem.* **1994**, *269*, 33082.
- Rosen, G. M.; Tsai, P.; Weaver, J.; Porasuphatana, S.; Roman, L. J.; Starkov, A. A.; Fiskum, G.; Pou, S. *J. Biol. Chem.* **2002**, *277*, 40275.
- Zhang, L.; Dawson, V. L.; Dawson, T. M. *Pharmacol. Ther.* **2006**, *109*, 33.
- Dorheim, M. A.; Tracey, W. R.; Pollock, J. S.; Grammas, P. *Biochem. Biophys. Res. Commun.* **1994**, *205*, 659.
- Norris, P. J.; Waldvogel, H. J.; Faull, R. L. M.; Love, D. R.; Emson, P. C. *Neuroscience* **1996**, *1037*, 72.
- Sims, N. R.; Anderson, M. F. *Neurochem. Int.* **2002**, *40*, 511.
- Calabrese, V.; Mancuso, C.; Calvani, M.; Rizzarelli, E.; Butterfield, D. A.; Stella, A. M. *Nat. Rev.* **2007**, *8*, 766.
- Hobbs, A. J.; Higgs, A.; Moncada, S. *Annu. Rev. Pharmacol. Toxicol.* **1999**, *39*, 191.
- Delker, S. L.; Ji, H.; Li, H.; Jamal, J.; Fang, J.; Xue, F.; Silverman, R. B.; Poulos, T. L. *J. Am. Chem. Soc.* **2010**, *132*, 5437.
- Ji, H.; Tan, S.; Igarashi, J.; Li, H.; Derrick, M.; Martásek, P.; Roman, L. J.; Vásquez-Vivar, J.; Poulos, T. L.; Silverman, R. B. *Ann. Neurol.* **2009**, *65*, 209.
- (a) Lawton, G. R.; Ranaivo, H. R.; Wing, L. K.; Ji, H.; Xue, F.; Martesek, P.; Roman, L. J.; Watterson, D. M.; Silverman, R. B. *Bioorg. Med. Chem.* **2009**, *17*, 2371; (b) Ji, H.; Delker, S. L.; Li, H.; Martasek, P.; Roman, L. J.; Poulos, T. L.; Silverman, R. B. *J. Med. Chem.* **2010**, *53*, 7804.
- Silverman, R. B. *The Organic Chemistry of Drug Design and Drug Action*, 2nd edition; Academic Press: San Diego, 2004.
- Xue, F.; Fang, J.; Lewis, W. W.; Martasek, P.; Roman, L. J.; Silverman, R. B. *Bioorg. Med. Chem. Lett.* **2010**, *20*, 554.
- Xue, F.; Huang, H.; Li, H.; Fang, J.; Poulos, T. L.; Silverman, R. B. *Bioorg. Med. Chem.* **2010**, *18*, 6526.
- Delker, S. L.; Xue, F.; Li, H.; Jamal, J.; Silverman, R. B.; Poulos, T. L. *Biochemistry* **2010**, *49*, 10803.
- Xue, F.; Li, H.; Fang, J.; Poulos, T. L.; Silverman, R. B. *J. Am. Chem. Soc.* **2010**, *132*, 14229.
- Xue, F.; Delker, S. L.; Li, H.; Fang, J.; Jamal, J.; Silverman, R. B.; Poulos, T. L. *J. Med. Chem.* **2011**, *54*, 2039.
- Fishlock, D.; Perdicakis, B.; Montgomery, H. J.; Guillemette, J. G.; Jervis, E.; Lajoie, G. A. *Bioorg. Med. Chem.* **2003**, *11*, 869.
- Yamanoi, K.; Ohfun, Y. *Tetrahedron Lett.* **1988**, *29*, 1181.
- Shimamoto, K.; Ishida, M.; Shinozaki, H.; Ohfun, Y. *J. Org. Chem.* **1991**, *56*, 4167.
- Kozikowski, A.; Raven Press: New York, 1993.
- Wermuth, C. G.; *The Practice of Medicinal Chemistry*; Academic Press: San Diego, 1996.
- Perrin, C. L.; Fabian, M. A.; Rivero, I. A. *Tetrahedron* **1999**, *55*, 5773.
- Pryde, D. C.; Cook, A. S.; Burring, D. J.; Jones, L. H.; Foll, S.; Platts, M. Y.; Sanderson, V.; Corless, M.; Stobie, A.; Middleton, D. S.; Foster, L.; Barker, L.; Graaf, P. V. D.; Stacey, P.; Kohl, C.; Coggon, S.; Beaumont, K. *Bioorg. Med. Chem.* **2007**, *15*, 142.
- Tchilibon, S.; Kim, S.-K.; Gao, Z.-G.; Harris, B. A.; Blaustein, J. B.; Gross, A. S.; Duong, H. T.; Melman, N.; Jacobson, K. A. *Bioorg. Med. Chem.* **2004**, *12*, 2021.
- Xue, F.; Kraus, J. M.; Jansen Labby, K.; Ji, H.; Mataka, J.; Xia, G.; Li, H.; Delker, S. L.; Roman, L. J.; Martásek, P.; Poulos, T. L.; Silverman, R. B. *J. Med. Chem.* **2011**, *54*, 6399.
- (a) Hevel, J. M.; White, K. A.; Marletta, M. A. *J. Biol. Chem.* **1991**, *266*, 22789; (b) Roman, L. J.; Sheta, E. A.; Martásek, P.; Gross, S. S.; Liu, Q.; Masters, B. S. *Proc. Natl. Acad. Sci. U.S.A.* **1995**, *92*, 8428; (c) Martasek, P.; Liu, Q.; Roman, L. J.; Gross, S. S.; Sessa, W. C.; Masters, B. S. *Biochem. Biophys. Res. Commun.* **1996**, *219*, 359.
- Hevel, J. M.; Marletta, M. A. *Method Enzymol.* **1994**, *233*, 250.
- McPhillips, T. M.; McPhillips, S. E.; Chiu, H. J.; Cohen, A. E.; Deacon, A. M.; Ellis, P. J.; Garman, E.; Gonzalez, A.; Sauter, N. K.; Phizackerley, R. P.; Soltis, S. M.; Kuhn, P. J. *Synchrotron Radiat.* **2002**, *9*, 401.
- Otwinowski, Z.; Minor, W. *Methods Enzymol.* **1997**, *276*, 307.
- Collaborative Computational Project Number 4, the CCP4 Suite: Programs for Protein Crystallography. *Acta Cryst.* **1994**, *D50*, 760.
- Murshudov, G. N.; Vagin, A. A.; Dodson, E. J. *Acta Cryst.* **1997**, *D53*, 240.
- Emsley, P.; Cowtan, K. *Acta Cryst.* **2004**, *D60*, 2126.
- Winn, M. D.; Isupov, M. N.; Murshudov, G. N. *Acta Cryst.* **2001**, *D57*, 122.